



Since January 2020 Elsevier has created a COVID-19 resource centre with free information in English and Mandarin on the novel coronavirus COVID-19. The COVID-19 resource centre is hosted on Elsevier Connect, the company's public news and information website.

Elsevier hereby grants permission to make all its COVID-19-related research that is available on the COVID-19 resource centre - including this research content - immediately available in PubMed Central and other publicly funded repositories, such as the WHO COVID database with rights for unrestricted research re-use and analyses in any form or by any means with acknowledgement of the original source. These permissions are granted for free by Elsevier for as long as the COVID-19 resource centre remains active.



Pharmaceutics, Drug Delivery and Pharmaceutical Technology

Aerosol Inhalation Delivery of Triazavirin in Mice: Outlooks for Advanced Therapy Against Novel Viral Infections



Sergey V. Valiulin^a, Andrey A. Onischuk^a, Sergey N. Dubtsov^a, Anatoly M. Baklanov^a,
Sergey V. An'kov^b, Maria E. Plokhotnichenko^a, Tatyana G. Tolstikova^b,
Galina G. Dultseva^{a,*}, Vladimir L. Rusinov^c, Valery N. Charushin^c, Vasily M. Fomin^d

^a Voevodsky Institute of Chemical Kinetics and Combustion, SB RAS, Novosibirsk 630090, Russia

^b Vorozhtsov Institute of Organic Chemistry, SB RAS, Novosibirsk 630090, Russia

^c Postovskii Institute of Organic Synthesis, UrB RAS, Yekaterinburg 620137, Russia

^d Khristianovich Institute of Theoretical and Applied Mechanics, SB RAS, Novosibirsk 630090, Russia

ARTICLE INFO

Article history:

Received 22 August 2020

Revised 18 November 2020

Accepted 18 November 2020

Available online 26 November 2020

Keywords:

Pulmonary drug delivery

Drug aerosol

Pharmacokinetics

Elimination rate

Bioavailability

Antiviral drug

Triazavirin

ABSTRACT

Under pandemic-caused emergency, evaluation of the potential of existing antiviral drugs for the treatment of COVID-19 is relevant. Triazavirin, an antiviral drug developed in Russia for per-oral administration, is involved in clinical trials against SARS-CoV-2 coronavirus. This virus has affinity to epithelial cells in respiratory tract, so drug delivery directly in lungs may enhance therapeutic effect and reduce side effects for stomach, liver, kidneys. We elaborated ultrasonic method of triazavirin aerosol generation and investigated the inhalation delivery of this drug in mice. Mean particle size and number concentration of aerosol used in inhalation experiments are 560 nm and $4 \times 10^5 \text{ cm}^{-3}$, respectively. Aerosol mass concentration is $1.6 \times 10^{-4} \text{ mg/cm}^3$. Inhalation for 20 min in a nose-only chamber resulted in 2 mg/kg body delivered dose and 2.6 $\mu\text{g/mL}$ triazavirin concentration in blood plasma. Elimination rate constant determined in aerosol administration experiments was $k_e = 0.077 \text{ min}^{-1}$, which agrees with the value measured after intravenous delivery, but per-oral administration resulted in considerably lower apparent elimination rate constant of pseudo-first order, probably due to non-linear dependence of absorption rate on triazavirin concentration in gastrointestinal tract. The bioavailability of triazavirin aerosol is found to be 85%, which is about four times higher than for per-oral administration.

© 2020 American Pharmacists Association[®]. Published by Elsevier Inc. All rights reserved.

Introduction

The SARS-CoV-2 coronavirus causes severe and even fatal symptoms, such as acute respiratory distress syndrome, requiring special treatment and more likely affecting elderly persons with comorbidities. The new pathogen is β -coronavirus, a large, enveloped, positive-stranded RNA virus. It is the seventh coronavirus known to infect humans and the third of highly pathogenic human coronaviruses, identified after the Middle East respiratory syndrome coronavirus (MERS-CoV) and severe acute respiratory syndrome coronavirus (SARS-CoV).

Many research groups are working now on different therapies for treatment or prevention of COVID-19. The time required to develop a new drug is too long, which is unacceptable in the context of current emergency case. Therefore, a great interest is

now focused on investigation of existing antiviral drugs to redirect them for treatment of this disease. Several antiviral drugs are now under investigation, predominately those which are active against various influenza sub-types and other RNA viruses. The list of these drugs includes favipiravir, umifenovir, triazavirin, baloxavir marboxil and others.^{1,2}

Triazavirin is an original antiviral drug developed in Russia. This substance is effective against a wide range of influenza viruses, including H5N1 strain.³⁻⁸ Due to similarity between H5N1 and SARS-CoV-2, triazavirin is considered as an option to combat SARS-CoV-2.^{1,9} Triazavirin $\text{C}_5\text{H}_4\text{N}_6\text{O}_3\text{S}$ (7-methylthio-3-nitro-6H-[1,2,4]triazolo[5,1-c][1,2,4]triazin-4-one) is an antiviral preparation of azoloazine family. This is a drug with rather low toxicity: $\text{LD}_{50} = 9.5 \text{ g/kg}$ for intragastric introduction in mice, while the oral introduction of triazavirin in dogs in the dose of 400 mg/kg (which is 20 times higher than the recommended daily dose for humans) was determined to cause no structural, physiological or behavioral changes.⁵ According to the results of acute toxicity tests, triazavirin is classified as practically non-toxic drug, and it does not exhibit

* Corresponding author.

E-mail address: dultseva@kinetics.nsc.ru (G.G. Dultseva).

cumulative toxicity. Trial with healthy volunteers revealed no substantial side effects. Side effects classified as very rare ones include dyspeptic disorders (meteorism, diarrhea), and contraindications are limited to renal and hepatic impairment.⁵ The maximal concentration of triazavirin in blood after the intake of 250 mg three times a day was 4.8 µg/mL. These data demonstrate that the therapeutic window of triazavirin is broad. This molecule has a core structurally close to guanine, one of the “letters” comprising DNA and RNA, which underlies the ability of triazavirin to interfere with the regulation of biosynthesis of purine nucleotides. Experimental observations suggest that triazavirin inhibits some enzymes involved in the vital cycle of viral proteins. Triazavirin was shown to demonstrate affinity to viral spike glycoproteins, thus inhibiting their tendency to bind the angiotensin-protecting enzyme 2 (ACE 2) and thus preventing fusion with host cells. Since the novel virus exhibits 10 times stronger binding with ACE 2 than, for example, SARS-CoV, drug action at this stage may be crucial for the successful therapy of COVID-19. It was demonstrated with the model of lethal influenza infection in mice that a substantial advantage of triazavirin with respect to other antiviral agents is its ability to protect animals from hemorrhagic pneumonia.⁵ These data, along with the results of clinical trial of triazavirin against influenza virus,⁵ paved the way to the clinical trial against SARS-CoV-2, which is carried out in Russia, to be completed in November 2020. Preliminary positive effect of triazavirin in the treatment of COVID-19 was obtained in the multicenter and blind randomized controlled clinical trial ongoing in China. This trial has already provided some evidence that triazavirin is efficient as a drug to treat COVID-19.¹⁰

Triazavirin is available as a drug for peroral administration in capsules. However, the oral bioavailability of triazavirin is only 20%, and absorption time is about 2 h. Therefore, other routes of administration with higher bioavailability and shorter absorption time are needed to decrease the cost of therapy and to enhance its efficiency.

The entry for SARS-CoV-2 virus is mouth or nose. Then it enters the alveolar region of lungs and binds with ACE2. As the novel virus has affinity to the epithelial cells of respiratory tract, drug delivery directly into lungs as the target organ may enhance the therapeutic effect, accompanied by a decrease in side effects for stomach, liver, kidneys etc. Therefore, the pulmonary administration of antiviral drugs may provide advantages with respect to the traditional oral dosage forms.

The pulmonary aerosol delivery is extensively used today to treat respiratory diseases such as asthma, emphysema, chronic obstructive pulmonary disease, cystic fibrosis, primary pulmonary hypertension, and cancer.¹¹⁻¹³ In recent decades the lung alveolar part is increasingly considered as a portal for the delivery of systemic aerosolized drugs because of large surface area, good vascularization and direct connection between pulmonary and systemic circulations.¹⁴⁻¹⁷ Lungs are very permeable for drugs because of ultra-thinness of alveolar epithelium and, therefore, this way of administration is comparable to intravenous injections. However, in contrast to injections, inhalation is non-invasive and therefore painless, and can be used by patients at home without the health-care staff.

The modern inhalers that are available on the market include three main groups: dose-metering systems, dry powder inhalers, and nebulizers.¹⁸ In our studies, we chose to use nebulizers to deliver the aerosol to laboratory animals because the former two kinds of inhalers have some specific features bringing some complications into their application for this purpose. In particular, pressurized dose-metering inhalers provide rather high aerosol velocity, which may result in an excessive oropharyngeal deposition. As far as dry powder inhalers are concerned, their application

in inhalation experiments may involve difficulties with reproducibility, because the dry powder formulation appears to be shelf life dependent, so aerosol properties become the functions of powder storage time. For these reasons, we chose nebulizers. Inhalation of drug solutions in a nebulizer combined with an inhalation device is an especially effective treatment. When using nebulizers people do not need to be able to breathe in forcefully, nor do they need any particular skill. This way of inhalation results in less of the medication deposited in the throat, and larger part reaches the lungs with respect to dose-metering and dry powder inhalers.

In our previous works we have studied the pulmonary delivery of aerosolized non-steroid anti-inflammatory,¹⁹⁻²¹ hypotensive,²² anti-tuberculous drugs.²³ The dependence of lung deposition efficiency and delivered dose on particle size was investigated. The deposition of drug nanoparticles in the respiratory tract was studied both experimentally (in mice) and theoretically through the simulation of aerosol flow aerodynamics in human respiratory tract. It was demonstrated in those works that the respiratory delivery is much more efficient than peroral administration of the studied drugs. For instance, indomethacin delivery in the form of aerosol (nanometer-sized particles) in mice required a therapeutic dose six orders of magnitude less than that for peroral administration, to achieve the same effect, which was assessed as analgesic action (measured with the help of the hot-plate test) and anti-inflammatory effect, quantified as a decrease in histamine-caused edema. The bioavailability of drugs was shown to be substantially higher in the case of respiratory delivery in comparison with peroral administration.¹⁹ The objective of this study was to investigate the aerosol delivery of triazavirin, which is expected to be an effective drug against SARS-CoV-2, using an ultrasonic nebulizing system.

Materials and Methods

Aerosol Generation and Inhalation Equipment

We used an ultrasonic nebulizer to generate the aerosol of triazavirin in a set-up shown in Fig. 1. The aerosol is generated by applying an alternating electric field to a piezoelectric transducer placed in contact with the aqueous solution of triazavirin to be nebulized. The transducer converts the electrical signal into periodic mechanical vibrations to create oscillatory pressure disturbances in the liquid with the frequency of 1.7 MHz and input power 30 W. These ultrasonic vibrations give rise to interfacial destabilization, which results in the formation of small droplets above the surface of the liquid. Air purified by passing through a filter is let into the vessel with the liquid, and aerosol consisting of the droplets of triazavirin aqueous solution comes out of the nebulizer.

The size of aerosol particles is an important parameter which determines the region of the pulmonary system where the particles are predominantly deposited. However, the use of liquid droplets for inhalation creates some problems as the size of nebulized droplets is changing due to evaporation when passing through the connecting tubes. Therefore, the original droplet size would be different from that inhaled. Evaporation rate depends on the relative humidity of surrounding gas. During inhalation experiment, relative humidity would change with time due to a progressive increase in water saturation of the surface of connecting tubes, thus creating problems in reproducibility of the dose inhaled by laboratory animals.

To avoid uncertainty of droplet size due to evaporation, aerosol particles are dried out before being supplied to the inhalation chamber. To this end, the aerosol flow is supplied to the desiccator, which consists of two concentric cylinders, an inner wire screen, and an outer metal tube. Desiccant silica gel beads are fixed between the wire screen and the outer tube. As the aerosol flow moves through

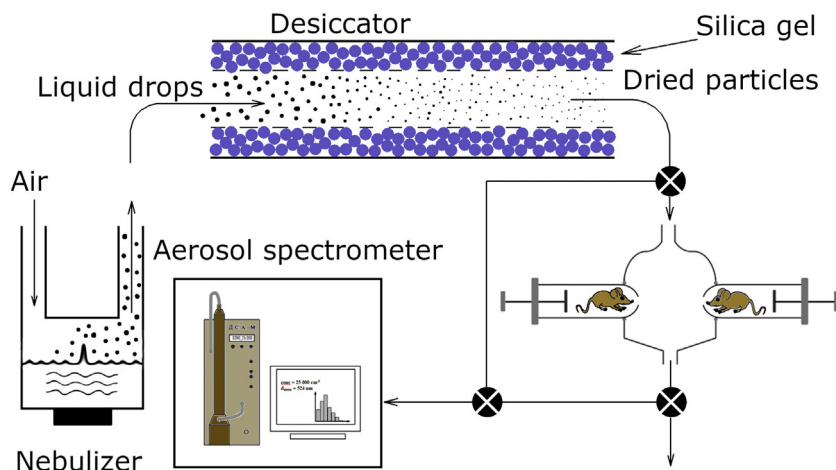


Fig. 1. Schematic of inhalation experiments.

the inner cylinder, water evaporates from the drops so that water vapor diffuses through the screen to be adsorbed by silica gel. The dried particles of triazavirin are coming out of the desiccator. The size of final aerosol particles depends on the concentration of triazavirin in the aqueous solution in nebulizer. Then the aerosol flow is supplied to a Nose Only (NO) mice inhalation chamber. A six-port chamber made of glass and metal is used. Mice are confined so that only the nose is exposed to the aerosol. Mice are placed radially around the cylindrical aerosol chamber. The inner diameter of the chamber is 6.0 cm. The triazavirin aerosol comes in and out through the axial pipes. All the mice are exposed to aerosol under identical conditions. The aerosol flow rate through the inhalation chamber is 2.5 L/min. The aerosol size and concentration in the inhalation chamber are monitored by a photoelectric counter and aerosol spectrometer.^{24–27} Both devices have been designed and built at the Institute of Chemical Kinetics and Combustion, Novosibirsk, Russia. The aerosol spectrometer is capable of measuring particle size distribution within the range 0.003–1.1 μm , and the photoelectric counter yields the size spectrum in the range 0.3–10 μm . Both devices are capable of measuring aerosol concentration within the range 10^1 – $5 \cdot 10^5 \text{ cm}^{-3}$ (without diluter). A three-cascade diluter is used to measure aerosol concentration in the range 10^5 – 10^9 cm^{-3} .²⁸

Sample Preparation and Chromatographic Analysis

Outbred laboratory male mice $28 \pm 3 \text{ g}$ in weight were used in inhalation experiments. Triazavirin concentrations in the samples of serum, lungs, kidneys, and liver were determined by means of high-performance liquid chromatography with a Milikrom A-02 instrument manufactured by Econova (Russia). The instrument is equipped with a column 7.5 cm long, filled with the reverse-phase sorbent ProntoSil C18. The column is thermostated at 40 °C. Blood samples were collected after decapitation in microtainer tubes and centrifuged at 3000 r.p.m. for 15 min, then 100 μL of serum from each sample was transferred into a centrifuge tube, and 33 μL of trifluoroacetic acid (50%, Fisher Chemical, 99+%, for HPLC) was added. The tubes were stirred for 5 min with Multi-Vortex V-32, then centrifuged for 15 min at a speed of 15,000 r.p.m. Supernatants (100 μL) were then sampled into chromatographic tubes. The volume of serum samples introduced into the chromatograph was 20 μL . Elution rate was 150 $\mu\text{L}/\text{min}$. Elution was carried out in the gradient mode: eluent A – acetonitrile (Sigma-Aldrich, for HPLC, gradient grade, $\geq 99.9\%$), eluent B – $2 \times 10^{-2} \text{ M}$ phosphate buffer (pH = 3). The initial concentration of eluent B – 3%, gradient –

0–600 μL – 3%, 600–1800 μL – 30%, 1800–2500 μL – 100%. Detection was carried out at the wavelengths of 254, 266, 280, 310 nm. The species of interest has maximal absorption at 266 nm. The lung, kidney or liver samples for analysis were homogenized with the addition of 0.9% NaCl solution for 60 s using a Q55 ultrasonic processor, and then analyzed in the same manner as blood samples.

All the animals were taken from SPF vivarium of Federal Research Center Institute of Cytology and Genetics of the Siberian Branch of Russian Academy of Sciences. Mice were housed in wire cages at 22–25 °C on a 12 h light-dark cycle. The animals had free access to standard pellet diet, tap water was available *ad libitum*. All the experimental procedures were approved by the Bio-Ethical Committee of the N.N. Vorozhtsov Novosibirsk Institute of Organic Chemistry of the Siberian Branch of Russian Academy of Sciences in accordance with the European Convention for the Protection of Vertebrate Animals used for Experimental and other Scientific Purposes 2010, and the requirements and recommendations of the Guide for the Care and Use of Laboratory Animals.

Results and Discussion

The total dose delivered by inhalation is measured as described in detail elsewhere.^{17–21} The total mass of particles deposited in the respiratory tract of one mouse per time t (min) can be written as

$$\Delta M = \alpha C_A F t \quad (1)$$

where C_A (g/cm^3) is the particle mass concentration in the aerosol chamber, F (cm^3/min) is the aerosol flow rate through the inhalation chamber. During the aerosol exposition only small fraction of particles from the aerosol stream in the inhalation chamber is deposited in the pulmonary ways of mice. Some fraction of particles comes through the chamber without being inhaled and some fraction is inhaled and then exhaled. To evaluate the pulmonary delivered dose one should take into account in Eq. (1) the mean fraction of particles α that were inhaled by one mouse from the aerosol stream and deposited in the pulmonary ways. The fraction α was measured as

$$\alpha = \frac{1}{N} \left(1 - \frac{n}{n_0} \right) \quad (2)$$

where N is the number of mice breathing simultaneously in the chamber, n and n_0 are the outlet aerosol number concentrations for

a chamber occupied with mice and for a non-occupied chamber, respectively. Substituting Eq. (2) into (1) we get

$$\Delta M = \left(1 - \frac{n}{n_0}\right) \frac{C_A Ft}{N} \quad (3)$$

Triazavirin aerosol for inhalation experiments was synthesized using an ultrasonic nebulizer (see Fig. 1). Fig. 2 shows the aerosol number concentration and mean diameter at the inlet of the inhalation chamber for different triazavirin solution concentrations in the nebulizer. The aerosol mass concentration was measured by sampling to the high-efficiency Whatman filter and weighing. Fig. 3 shows the aerosol mass concentration vs. triazavirin solution concentration. One can see from Fig. 2b that the particle diameter increases with the solution concentration in the nebulizer. This kind of dependence is expectable, because the increase of solution concentration results in the increase of mass of triazavirin in a drop, and, as a consequence, in the increase of the mean diameter of triazavirin particles after desiccation of droplets. The increase of triazavirin particle number concentration with the concentration of solution (Fig. 2a) is probably due to the dependence of the particle-to-wall deposition in the desiccator and other aerosol tracts on the particle diameter. The collateral increase of triazavirin particle number concentration and diameter gives the nonlinear increase of the triazavirin aerosol mass concentration at the inlet of inhalation chamber.

A typical size spectrum of triazavirin aerosol particles measured by the optical counter for triazavirin concentration 20 mg/mL is shown in Fig. 4. The solution of that concentration was used in all the subsequent inhalation experiments. To determine inhalation time necessary to deliver the therapeutic dose to laboratory animals, triazavirin concentration in the blood vs. inhalation time was measured as shown in Fig. 5. Together with inhalation time, the accumulated dose is given in the top axis. The blood was collected immediately after inhalation experiment. In these experiments,

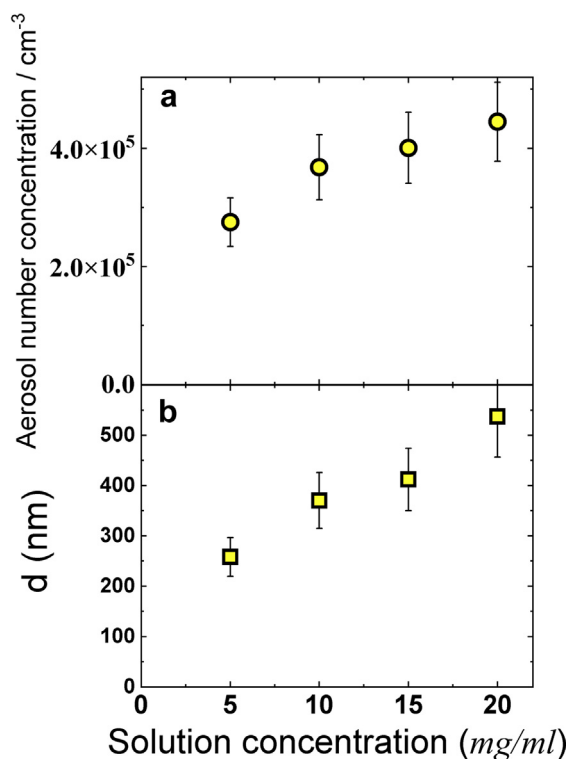


Fig. 2. Aerosol number concentration (a) and mean diameter (b) at the inlet of the inhalation chamber as a function of triazavirin solution concentration in the nebulizer.

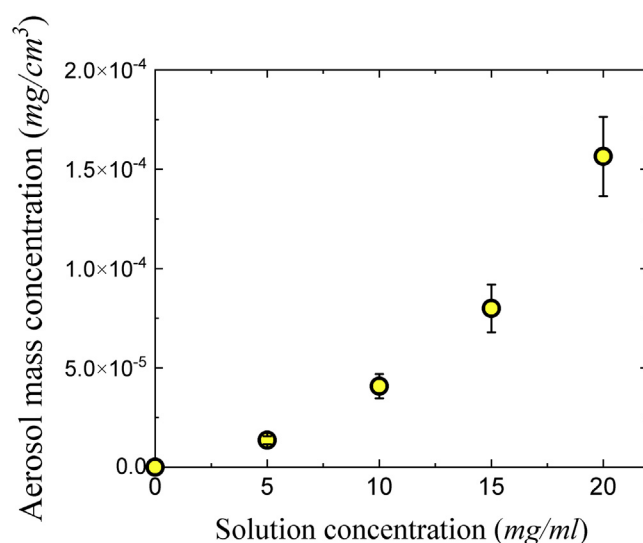


Fig. 3. Aerosol mass concentration versus triazavirin solution concentration.

triazavirin concentration in blood is controlled by both the rate of triazavirin elimination and the rate of administration to the body. The kinetics of triazavirin elimination can be described in terms of one-compartmental model:

$$dM/dt = w_a - k_e M \quad (4)$$

where M is the total mass of triazavirin in the body, w_a is the rate of triazavirin administration by inhalation, k_e is the first-order elimination rate constant. The total mass M is related to the triazavirin concentration C as measured in the blood plasma via the following equation

$$M = V_d \cdot C \quad (5)$$

where V_d is the volume of distribution, i.e. the theoretical volume that would be necessary to contain the total amount of an administered drug at the same concentration as that observed in the blood plasma. The combination of Eqs. (4) and (5) results in

$$dC/dt = w_a/V_d - k_e \cdot C \quad (6)$$

The solution of Eq. (6) is

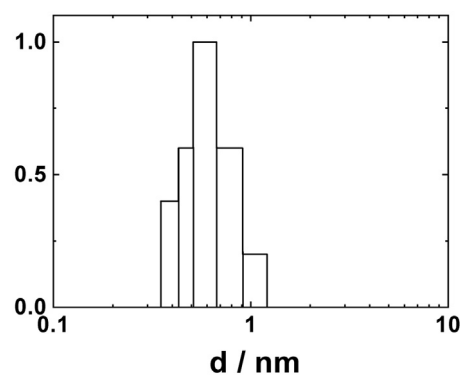


Fig. 4. Size distribution of triazavirin aerosol particles measured by the optical counter.

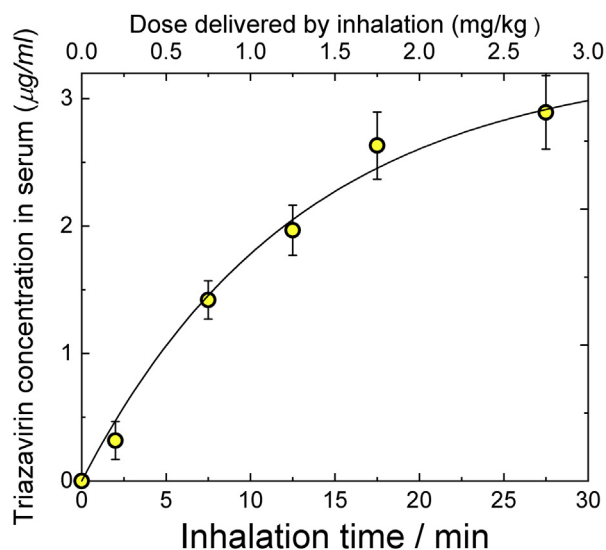


Fig. 5. Triazavirin concentration in serum vs. inhalation time. Solid line follows Eq. (7) with $k_e = 0.077 \text{ min}^{-1}$.

$$C = (1 - \exp(-k_e \cdot t)) \cdot w_a / (V_d \cdot k_e) \quad (7)$$

The experimental kinetics is well approximated by Eq. (7) with $k_e = 0.077 \pm 0.010 \text{ min}^{-1}$ and $w_a / (V_d \cdot k_e) = 3.31 \text{ µg mL}^{-1}$. As can be seen from Fig. 5, the rate of dose accumulation is $w_a = 100 \text{ µg/(kg min)}$, therefore, one can estimate $V_d = 390 \text{ mL/kg}$. The total volume of plasma in mice is about 35 mL per kg of body weight, i.e. V_d is about 10 times larger than the total volume of plasma.

Fig. 6 shows the dependence of triazavirin concentration in serum vs. delay time (i.e. time between the end of inhalation and sacrifice). The experiment was arranged as follows. The mice were exposed to triazavirin aerosol in the inhalation chamber for 20 min, which corresponded to the inhalation dose of 2 mg per kg of body weight. Then the inhalation was stopped and the mice were placed in special boxes for some delay time. Afterwards the animals were sacrificed and their blood was sampled. The concentration of triazavirin in plasma vs. delay time is well described by the first-order

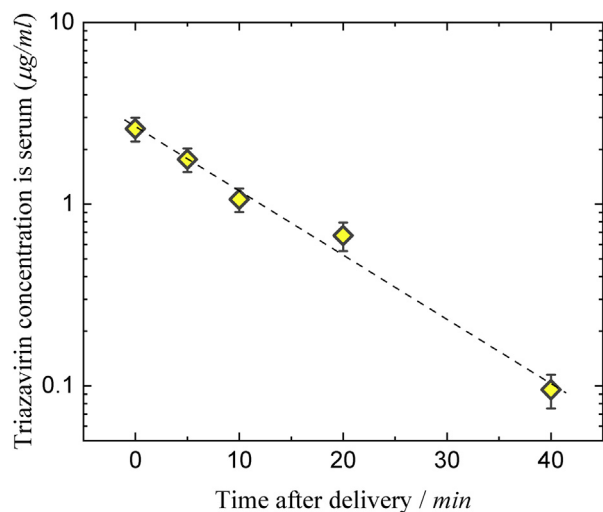


Fig. 6. Triazavirin concentration in serum vs. delay time (time between the end of inhalation and sacrifice). Dashed line corresponds to the first-order kinetics with the elimination rate constant $k_e = 0.077 \text{ min}^{-1}$. Inhalation dose is 2.0 mg/kg.

kinetics with the elimination rate constant $k_e = 0.077 \pm 0.010 \text{ min}^{-1}$ in agreement with that obtained in the dose accumulation experiments (Fig. 5). It was found that the accumulation of triazavirin in liver and kidneys is insignificant in inhalation experiments (as well as in the cases of intravenous and per-oral delivery). The mass of triazavirin in liver and kidneys proved to be less than 0.1 µg (on average) after inhalation for 20 min and the amount of triazavirin accumulated in lungs was within the range 0.2–0.4 µg (per one lung). After intravenous administration, the amount detected in lungs was 0.04–0.3 µg, while after peroral introduction it was about 0.06 µg. These data suggest that inhalation delivery of triazavirin provides the possibility of both systemic and local treatment (which is not less efficient than that in the case of intravenous administration and much more efficient than in the case of peroral intake).

It is also of interest to compare pharmacokinetic dependencies for aerosol delivery with those for intravenous and per-oral administrations. The intravenous injection (Fig. 7) results in the first-order kinetics for triazavirin in plasma with the elimination rate constant $k_e = 0.087 \pm 0.010 \text{ min}^{-1}$, which is in a reasonable agreement with that for aerosol administration.

In the case of per-oral administration, the temporal dependence of triazavirin concentration in plasma passes through the maximum (Fig. 8) which means that the absorption rate is a function of triazavirin concentration in the gastrointestinal (GI) region. The dependence of concentration on time can be described in terms of a two-compartmental model with the kinetics equations

$$\frac{dM_{GI}}{dt} = -k_{\alpha} M_{GI} \quad (8)$$

$$\frac{dM_B}{dt} = k_{\alpha} M_{GI} - k_{\beta} M_B \quad (9)$$

where M_{GI} is the mass of triazavirin in the GI region and M_B is that in the body beyond the gastrointestinal barrier; k_{α} and k_{β} are the apparent pseudo-first-order rate constants of absorption and elimination, respectively. The solution of Eqs. (8) and (9) is

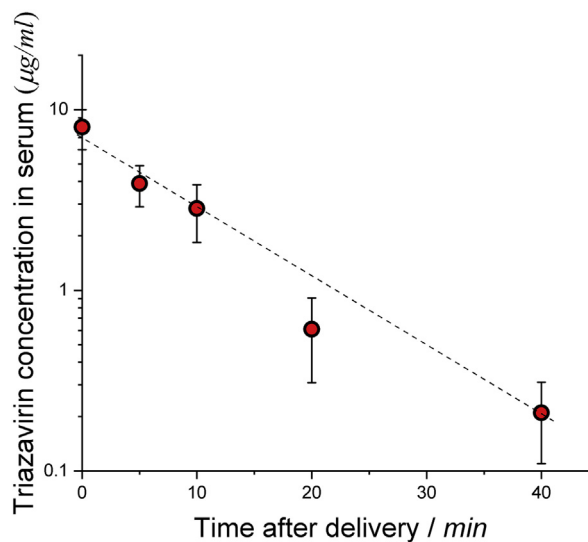


Fig. 7. Triazavirin concentration in serum vs. time (intravenous administration). Body delivered dose is 2.0 mg/kg. Dashed line corresponds to the first-order kinetics with the elimination rate constant $k_e = 0.087 \text{ min}^{-1}$.

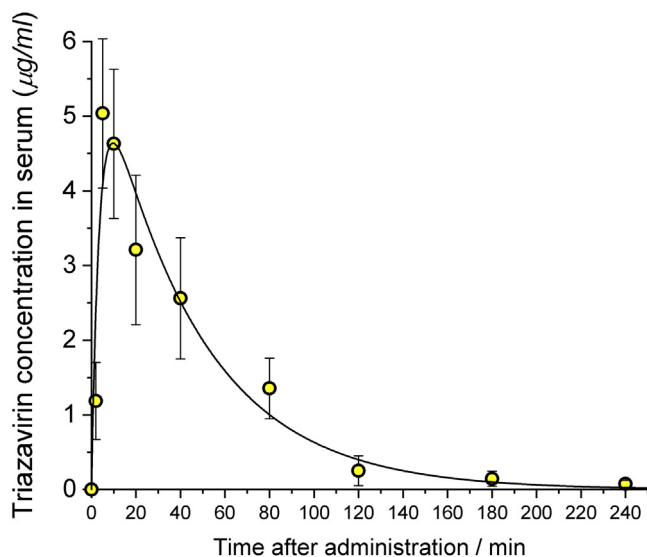


Fig. 8. Triazavirin concentration in serum vs. time (per-oral administration). Solid line follows Eq. (11). Body delivered dose is 30 mg/kg.

$$M_B = \frac{k_\alpha M_{GI}^0}{k_\beta - k_\alpha} (\exp(-k_\alpha t) - \exp(-k_\beta t)) \quad (10)$$

or

$$C = \frac{k_\alpha M_{GI}^0}{V_d(k_\beta - k_\alpha)} (\exp(-k_\alpha t) - \exp(-k_\beta t)) \quad (11)$$

where C is triazavirin concentration in serum, M_{GI}^0 is the initial mass of triazavirin in the GI region. Eq. (11) fits well the experimental concentration–time data plotted in Fig. 8, with k_α and k_β equal to 0.28 ± 0.03 and $0.023 \pm 0.003 \text{ min}^{-1}$, respectively. The quantity k_β is considerably less than the elimination rate constant k_e as

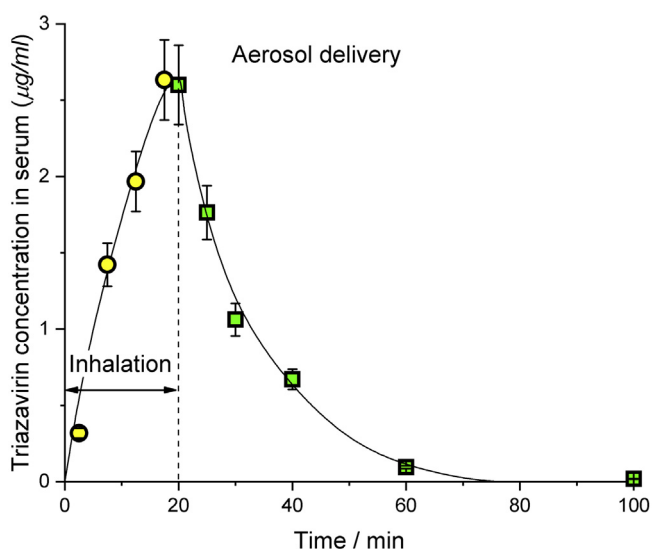


Fig. 9. Triazavirin concentration in serum vs. time (aerosol administration). Diamonds show an increase in concentration during inhalation (see also Fig. 5), squares – concentration decay after inhalation. The body delivered dose after inhalation for 20 min is 2.0 mg/kg.

determined in the intravenous and aerosol administration experiments. The reason is probably in non-linear dependence of the absorption rate on triazavirin concentration in the GI region.

The bioavailability F_A and F_{PO} of the aerosol and peroral forms of triazavirin, respectively, can be calculated as

$$F_A = \frac{AUC_A Dose_{IV}}{AUC_{IV} Dose_A} 100\% \quad (12)$$

$$F_{PO} = \frac{AUC_{PO} Dose_{IV}}{AUC_{IV} Dose_{PO}} 100\% \quad (13)$$

where AUC_A , AUC_{PO} and AUC_{IV} are the areas under the plasma concentration–time curves for the aerosol, per-oral and intravenous delivery, respectively, and $Dose_A$, $Dose_{PO}$ and $Dose_{IV}$, are the body delivered doses for these ways of administration. To calculate the bioavailability, the dependence of plasma concentration on total time (including both the inhalation time and the time after the inhalation) is plotted in Fig. 9. It is easy to calculate from the data shown in Figs. 7–9 the quantities $F_A = 85 \pm 15\%$ and $F_{PO} = 21 \pm 5\%$.

Conclusions

Aerosol inhalation delivery of triazavirin to the outbred male mice is investigated. For this purpose, an ultrasonic way of generation is elaborated. The mean size and concentration of aerosol generated from the aqueous solution of triazavirin, with the concentration of 20 mg/mL in the nebulizer, are 560 nm and $4 \times 10^5 \text{ cm}^{-3}$, respectively, which corresponds to the aerosol mass concentration $1.6 \times 10^{-4} \text{ mg cm}^{-3}$. After inhalation for 20 min in the nose-only chamber, the aerosol dose delivered to the laboratory animals proved to be 2 mg/kg, and triazavirin concentration in the blood plasma is found to be 2.6 µg/mL. The elimination rate constant was determined in aerosol administration experiments $k_e = 0.077 \text{ min}^{-1}$ to be in agreement with that measured after intravenous delivery, but per-oral administration resulted in considerably lower apparent elimination rate constant of pseudo-first order, probably due to non-linear dependence of the absorption rate on the triazavirin concentration in the GI region. It is found that aerosol administration, as well as intravenous and per-oral delivery, does not result in triazavirin accumulation in organs. The mass of triazavirin in liver and kidneys proved to be less than 0.1 µg (on average) after inhalation for 20 min and the amount of triazavirin accumulated in lungs was within the range 0.2–0.4 µg (per one lung). After intravenous administration, the amount detected in lungs was 0.04–0.3 µg, while after peroral introduction it was about 0.06 µg. These data suggest that inhalation delivery of triazavirin provides the possibility of both systemic and local treatment (which is not less efficient than that in the case of intravenous administration and much more efficient than in the case of peroral intake). The bioavailability of the aerosol form of triazavirin is found to be 85%, which is nearly four times larger than that for the traditional per-oral administration.

Conflicts of Interest

The authors declare no conflict of interest.

Acknowledgment

This research was funded by the Russian Science Foundation (Project No. 19-73-10143).

References

1. Lythgoe MP, Middleton P. Ongoing clinical trials for the management of the COVID-19 pandemic. *Trends Pharmacol Sci.* 2020;41(6):363-382.
2. Vincent MJ, Bergeron E, Benjannet S, et al. Chloroquine is a potent inhibitor of SARS coronavirus infection and spread. *Virology.* 2005;2(69):1-10.
3. Kiselev OI, Deeva EG, Mel'nikova TI, et al. A new antiviral drug Triazavirin: results of phase II clinical trial. *Vopr Virusol.* 2012;57(6):9-12.
4. Shvetsov A, Zabrodskaya Y, Nekrasov P, Egorov V. Triazavirine supramolecular complexes as modifiers of the peptide oligomeric structure. *J Biomol Struct Dyn.* 2018;36:2694-2698.
5. Deeva EG, Kiselev OI, Melnikova TI, et al. New antiviral drug Triazavirin. Results of phase I clinical trial. *Epidemiol Infect Dis.* 2013;20-26.
6. Loginova SY, Borisevich SV, Maksimov VA, et al. The study of antiviral activity of Triazavirin in relation to the influenza virus A(H5N1) (causative agent of influenza) on cellular culture. *Antibiot Chemother.* 2007;52(11-12):18-20.
7. Tikhonova EP, Kuz'mina TYu, Andronova NV, Tyushevskaya OA, Elistratova TA, Kuz'min AE. Study of effectiveness of antiviral drugs (umifenovir, triazavirin) against acute respiratory viral infections. *Kazan Med J.* 2018;99(2):215-223.
8. Karpenko I, Deev S, Kiselev O, et al. Antiviral properties, metabolism, and pharmacokinetics of a novel Azolo-1,2,4-triazine-derived inhibitor of influenza A and B virus replication. *Antimicrob Agents Chemother.* 2010;54:2017-2022.
9. Drugbank white paper, COVID-19: finding the right fit, identifying potential treatments using a data-driven approach. Available at: https://drugbank.s3-us-west-2.amazonaws.com/assets/blog/COVID-19_Web.pdf. Accessed May 12, 2020.
10. Wu X, Yu K, Wang Y, et al. The efficacy and safety of triazavirin for COVID-19: a trial protocol. *Engineering.* 2020. <https://doi.org/10.1016/j.eng.2020.06.011>.
11. Bailey MM, Berkland CJ. Nanoparticle formulations in pulmonary drug delivery. *Med Res Rev.* 2009;29:196-212.
12. Ruge CA, Kirch J, Lehr C-M. Pulmonary drug delivery: from generating aerosols to overcoming biological barriers - therapeutic possibilities and technological challenges. *Lancet Respir Med.* 2013;1:402-413.
13. Gagnadoux F, Pape AL, Lemarie E, et al. Aerosol delivery of chemotherapy in an orthotopic model of lung cancer. *Eur Respir J.* 2005;26:657-661.
14. Laube BL. The expanding role of aerosols in systemic drug delivery, gene therapy, and vaccination. *Respir Care.* 2005;50:1161-1176.
15. Agu RU, Ugwoke MI, Armand M, Kinget R, Verbeke N. The lung as a route for systemic delivery of therapeutic proteins and peptides. *Respir Res.* 2001;2:198-209.
16. Patton JS, Fishburn CS, Weers JG. The lungs as a portal of entry for systemic drug delivery. *Proc Am Thorac Soc.* 2004;1:338-344.
17. Labiris NR, Dolovich MB. Pulmonary drug delivery. Part I: physiological factors affecting therapeutic effectiveness of aerosolized medications. *J Clin Pharmacol.* 2003;56:588-599.
18. Hickey AJ, ed. *Pharmaceutical Inhalation Aerosol Technology.* New York: Marcel Dekker, Inc; 2004.
19. Onischuk AA, Tolstikova TG, Sorokina IV, et al. Anti-inflammatory effect from indomethacin nanoparticles inhaled by male mice. *J Aerosol Med Pulm Drug Deliv.* 2008;21:231-244.
20. Onischuk AA, Tolstikova TG, Sorokina IV, et al. Analgesic effect from ibuprofen nanoparticles inhaled by male mice. *J Aerosol Med Pulm Drug Deliv.* 2009;22:245-253.
21. Onischuk AA, Tolstikova TG, An'kov SV, et al. Ibuprofen, indomethacin and diclofenac sodium nanoaerosol: generation, inhalation delivery and biological effects in mice and rats. *J Aerosol Sci.* 2016;100:164-177.
22. Onischuk AA, Tolstikova TG, Baklanov AM, et al. Generation, inhalation delivery and anti-hypertensive effect of nisoldipine nanoaerosol. *J Aerosol Sci.* 2014;78:41-54.
23. Valiulin SV, Onischuk AA, Baklanov AM, et al. Excipient-free isoniazid aerosol administration in mice: evaporation-nucleation particle generation, pulmonary delivery and body distribution. *Int J Pharm.* 2019;563:101-109.
24. Ankilov A, Baklanov A, Colhoun M, et al. Intercomparison of number concentration measurements by various aerosol particle counters. *Atmos Res.* 2002;62:177-207.
25. Dubtsov S, Ovchinnikova T, Valiulin S, et al. Laboratory verification of Aerosol Diffusion Spectrometer and the application to ambient measurements of new particle formation. *J Aerosol Sci.* 2017;105:10-23.
26. Onischuk AA, Baklanov AM, Valiulin SV, Moiseenko PP, Mitrochenko VG. Aerosol diffusion battery: the retrieval of particle size distribution with the help of analytical formulas. *Aerosol Sci Technol.* 2018;52:165-181.
27. Onischuk AA, Valiulin SV, Baklanov AM, Moiseenko PP, Mitrochenko VG. Determination of the aerosol particle size distribution by means of the diffusion battery: analytical inversion. *Aerosol Sci Technol.* 2018;52:841-853.
28. Onischuk AA, Vosel SV, Borovkova OV, Baklanov AM, Karasev VV, diStasio S. Experimental study of homogeneous nucleation from the bismuth supersaturated vapor: evaluation of the surface tension of critical nucleus. *J Chem Phys.* 2012;136:224506.